ELSEVIER

Inorganica Chimica Acta 224 (1994) 113–124

Inorganica Chimica Acta

Rotation and orientation of axially coordinated imidazoles in low-spin ferric porphyrin complexes

Mikio Nakamura[a,*], Kunihiko Tajima[b], Kohji Tada[b], Kazuhiko Ishizu[b], Nobuo Nakamura[c]

[a]*Department of Chemistry, Toho University School of Medicine, Ota-ku, Tokyo 143, Japan*
[b]*Department of Chemistry, Faculty of Science, Ehime University, Matuyama 790, Japan*
[c]*Department of Chemistry, Faculty of Science, University of Tokyo, Bunkyo-ku, Tokyo 113, Japan*

Received by Editor 12 August 1993; revised by Publisher 24 May 1994

Abstract

The variable temperature ^{1}H NMR spectra of a series of low-spin bis(imidazole)tetrakis(2,4,6-trialkylphenyl)porphinatoiron(III) chlorides, (R-TPP)Fe(L)$_2$Cl, showed that the rotation of axially coordinated 2-alkyl- and benzimidazoles slowed down on the NMR time scale at low temperature to give four pyrrole signals. The ^{13}C NMR spectra of the ^{13}C enriched (Me-TPP)Fe(2-methylimidazole)$_2$Cl at the *meso* positions gave two *meso* signals with equal intensity at the temperature range below −25 °C. These results indicate that each of the axial ligands is perpendicularly aligned over a diagonal C_{meso}–Fe–C_{meso} axis. The shift range of the pyrrole protons reached as much as 12 ppm at −56 °C. The apparent unfavorable orientation of the ligands was explained in terms of the S_4 deformed structure of the porphinatoiron core in solution. The relatively small slopes in Curie plots of the pyrrole-H and the *meso* ^{13}C signals were also ascribed to the deformed structure of the core. In the mixed ligand complexes having a hindered 2-isopropylimidazole and an unhindered 1-methylimidazole ligand, it was suggested from the ^{1}H and ^{13}C NMR splitting patterns that the rotation of only one of the ligands, 2-isopropylimidazole, was frozen. In these complexes the spread of the pyrrole signals increased to nearly 20 ppm. The activation free energies for rotation were determined by the dynamic NMR technique. They changed in the range of 11.3 to 13.6 kcal mol^{-1} depending upon the bulkiness of the axial ligands and *o*-alkyl substituents. Close examination of the dynamic process using the saturation transfer technique revealed that the dissociation of the axial ligands occurred concomitantly during the rotation process in the case of the bis(2-isopropylimidazole) complexes. In contrast, pure rotation process was observed in the complexes with 2-methyl-, 2-ethyl-, 1,2-dimethyl- and benzimidazole. X band ESR spectra of these complexes were taken at 4.2 K in CH_2Cl_2 glass. Although complexes with perpendicularly aligned planar ligands tend to exhibit so called 'strong g_{max}' type signals, the complexes studied here showed signals with smaller g_z values.

Keywords: NMR study; Iron complexes; Porphyrin complexes

1. Introduction

Spectral properties such as NMR [1,2] and ESR [3,4] of naturally occurring heme proteins are controlled by various factors. In the case of heme proteins carrying at least one histidine group as axial ligand, orientation of the ligand relative to the heme plane is considered to be one of the factors [5]. This is because, as La Mar and Walker [1] pointed out, p(π) orbitals of histidine (L) can interact with degenerate d(π) orbitals of iron (M) in L to M π-donation mode and raise the energy levels of the two orbitals to a different extent. In an extreme case where the imidazole ligand of histidine is placed along one of the diagonal N–Fe–N axes (x axis), the p(π) orbitals interact solely with a d_{yz} orbital and raise its energy level. As a result, an unpaired electron is placed in the d_{yz} orbital and transferred to the pyrrole rings along the y axis by interaction with the porphyrin 3e(π) orbital. Since this orbital has large spin densities on nitrogens and pyrrole β-carbons, the pyrrole methyl protons along the y axis appear at lower magnetic field than those along the x axis in the ^{1}H NMR spectra [6–9]. A large energy difference between the d_{yz} and d_{zx} orbitals would also

*Corresponding author.

SSDI 0020-1693(94)04115-C

give highly rhombic signals in the ESR spectra [10,11]. In contrast, if two histidine ligands are placed perpendicularly to each other above and below the porphyrin ring, the energy levels of both the d_{yz} and d_{zx} orbitals are equally raised. In this case, four methyl protons should show similar isotropically shifted signals, since all the pyrrole carbons are expected to have similar spin densities. In the ESR spectra, the complexes with perpendicularly aligned planar axial ligands usually give so called 'strong g_{max}' type signals [12–18]. The fixed orientation of planar histidine ligands, therefore, affects both NMR and ESR spectral properties. It is difficult, however, to determine how much the effect contributes to the observed spectral properties, since hemes are located in highly unsymmetrical cavities of proteins; the chemical shifts of the peripheral protons are influenced by hydrogen bonding, steric repulsion and non-bonded attractive interactions between the heme and protein. Thus, in order to elucidate the orientation effect of the axial planar ligands, suitable iron complexes of synthetic porphyrins are necessary in which rotation of the coordinated imidazole ligands is hindered.

Restriction of imidazole rotation in low-spin ferric complexes has been examined by several groups [19–21]. Traylor and Berzinis [19] prepared a complex in which the imidazole ligand is fixed by covalent attachment to the protoporphyrin IX periphery. The peripheral methyl protons exhibited a fairly large spread, 17.1 ppm at an ambient temperature, as in the case of some heme proteins such as horse heart cytochrome *c* [22] and pig liver cytochrome b_5 [23]. Quite recently, Walker and co-workers reported some model complexes in which unhindered imidazole ligands are fixed due to hindered rotation [24,25]. Such examples are bis(1-methylimidazole) complexes of mono-*ortho*-substituted tetraphenylporphinatoiron(III) chlorides where *o*-substituents are $-CONR_2$ with bulky alkyl groups. These complexes showed eight signals for pyrrole protons at an ambient or low temperature. The shift range of one of the complexes reached as much as 14 ppm at -23 °C.

We have reported for the first time that the rotation of sterically hindered imidazole ligands such as 2-methylimidazole and 1,2-dimethylimidazole in low-spin bis(imidazole)tetramesitylporphinatoiron(III) chloride slowed down on the NMR time scale at low temperatures to show perpendicularly fixed alignment of the ligands [26,27]. These complexes are quite suitable for elucidating the orientation effects on the physicochemical properties, since the pyrrole protons in these complexes become non-equivalent only when the rotation of the axial ligands is hindered. The purpose of this paper is to present the NMR and ESR spectral properties of a series of bis(imidazole)tetrakis(2,4,6-trialkylphenyl)porphinatoiron(III) chlorides, carrying rotationally fixed 2-alkylimidazoles and benzimidazole, and to discuss the relationship between the ligand orientation and spectral properties of the complexes.

2. Experimental

2.1. Materials and abbreviations

2,4,6-Trialkylbenzaldehydes were prepared by the reaction of 1,3,5-trialkylbenzene and dichloromethyl methyl ether in the presence of $TiCl_4$ [28,29]. Imidazole derivatives such as imidazole (HIm), 1-methylimidazole (1-MeIm), 2-methylimidazole (2-MeIm), 2-ethylimidazole (2-EtIm), 2-isopropylimidazole (2-^{i}PrIm), 1,2-dimethylimidazole (1,2-Me_2Im) and benzimidazole (BzIm) were purchased from Tokyo Kasei Kogyo Co., Ltd. or Aldrich Chemical Company, Inc. and they were further purified either by distillation or by recrystallization. 1-Methyl-2-isopropylimidazole (1-Me-2-^{i}PrIm) [30] was prepared by the methylation of 2-^{i}PrIm using dimethyl sulfate followed by a continuous ether extraction from the alkali solution, and was purified by distillation at 70–72 °C (1 mmHg). ^{1}H NMR ($CDCl_3$): 1.32 (d, 6H, $J=6.8$ Hz), 3.00 (m, 1H, $J=6.8$ Hz), 3.59 (s, 3H), 6.75 (d, 1H, $J=1.3$ Hz), 6.92 (d, 1H, $J=1.3$ Hz).

2.1.1. Free base porphyrins, (R-TPP)H_2

meso-Tetrakis(2,4,6-trimethylphenyl)porphyrin, (Me-TPP)H_2, was prepared according to Lindsey and co-workers by the condensation reaction of 2,4,6-trimethylbenzaldehyde with pyrrole in the presence of BF_3 etherate [31,32]. *meso*-Tetrakis(2,4,6-triethylphenyl)porphyrin, (Et-TPP)H_2, was similarly prepared from 2,4,6-triethylbenzaldehyde and freshly distilled pyrrole. *Anal.* Calc. for $C_{68}H_{78}N_4 \cdot (CH_2Cl_2)_{0.36}$: C, 83.61; H, 8.08; N, 5.71. Found: C, 83.62; H, 8.32; N, 5.55%. ^{1}H NMR ($CDCl_3$): -2.5 (broad s, 2H, NH), 0.62 (t, 24H, $J=7.8$ Hz, *o*-CH_2CH_3), 1.43 (t, 12H, $J=7.8$ Hz, *p*-CH_2CH_3), 2.05 (q, 16H, $J=7.8$ Hz, *o*-CH_2CH_3), 2.91 (q, 8H, $J=7.8$ Hz, *p*-CH_2CH_3), 7.22 (s, 8H, *m*-H), 8.50 (s, 4H, Py–H), 8.58 (s, 4H, Py–H). Visible (CH_2Cl_2): λ_{max} (log ϵ), 420 (5.92), 516 (4.34), 550 (3.86), 592 (3.76), 648 (3.49). *meso*-Tetrakis(2,4,6-triisopropylphenyl)porphyrin, (^{i}Pr-TPP)H_2, was similarly prepared from 2,4,6-triisopropylbenzaldehyde and pyrrole. *Anal.* Calc. for $C_{80}H_{102}N_4 \cdot (CH_2Cl_2)_{0.17}$: C, 84.90; H, 9.10; N, 4.94. Found: C, 84.85; H, 9.32; N, 5.00%. ^{1}H NMR ($CDCl_3$), 0.79 (d, 48H, $J=6.8$ Hz, *o*-$CH(CH_3)_2$), 1.46 (d, 24H, $J=6.8$ Hz, *p*-$CH(CH_3)_2$), 2.20 (m, 8H, $J=6.8$ Hz, *o*-$CH(CH_3)_2$), 3.18 (m, 4H, $J=6.8$ Hz, *p*-$CH(CH_3)_2$), 7.32 (s, 8H, *m*-H), 8.52 (s, 8H, Py–H). Visible (CH_2Cl_2): λ_{max} (log ϵ), 421 (5.80), 518 (4.26), 552 (3.91), 594 (3.72), 651 (3.61). The *meso* ^{13}C (99% ^{13}C) enriched (H-TPP)H_2 and (Me-TPP)H_2 were similarly prepared

using ^{13}C enriched benzaldehyde and 2,4,6-trimethylbenzaldehyde, respectively.

2.1.2. High-spin ferric porphyrins, (R-TPP)FeCl

A series of *meso*-tetrakis(2,4,6-trialkylphenyl)-porphinatoiron(III) chlorides, (R-TPP)FeCl, were prepared by refluxing a DMF solution of (R-TPP)H_2 with iron(II) chloride [33,34]. Some spectral data at 25 °C are described below. (Me-TPP)FeCl: ^1H NMR ($CDCl_3$, 25 °C): 3.9 (12H, *o*-CH_3), 6.6 (12H, *o*-CH_3), 4.17 (12H, *p*-CH_3), 14.3 (4H, *m*-H), 15.8 (4H, *m*-H), 79 (8H, pyrrole-H). (Et-TPP)FeCl: ^1H NMR ($CDCl_3$): 2.42 (12H, *p*-CH_2CH_3), 4.21 (8H, *p*-CH_2CH_3), 14.0 (4H, *m*-H), 15.8 (4H, *m*-H), 80 (8H, pyrrole-H). Visible (CH_2Cl_2): λ_{max} (log ϵ), 422 (5.11), 511 (4.26), 578 (3.69), 665 (3.53), 685 (3.54). (^{i}Pr-TPP)FeCl: ^1H NMR ($CDCl_3$, 25 °C): 2.2 (24H, *p*-$CH(CH_3)_2$), 4.1 (4H, *p*-$CH(CH_3)_2$), 13.9 (4H, *m*-H), 15.1 (4H, *m*-H), 80 (8H, pyrrole-H). Visible (CH_2Cl_2): λ_{max} (log ϵ), 415 (4.99), 512 (4.11), 575 (3.53), 675 (3.38), 703 (3.40).

2.1.3. Low-spin bis(imidazole) complexes, (R-TPP)-Fe(L)$_2$Cl

A high-spin ferric porphyrin complex was converted into the corresponding low-spin complex in an NMR sample tube by the addition of 6 equiv. of imidazole as a $CDCl_3$ or CD_2Cl_2 solution. Some of the high-spin complexes exhibited no conversion into the low-spin complexes at 25 °C even in the presence of 6 equiv. of ligand. Most of them, however, showed spin conversion at least partially at lower temperatures. The series of low-spin bis(imidazole) complexes examined in this study are abbreviated as (R-TPP)Fe(L)$_2$Cl where R is methyl (Me), ethyl (Et) or isopropyl (^{i}Pr) and L is the axial imidazole ligand such as HIm, 1-MeIm, 2-MeIm, 2-EtIm, 2-^{i}PrIm, 1,2-Me_2Im, 1-Me-2-^{i}PrIm and BzIm.

2.2. Spectral measurement

Samples for NMR measurement were prepared under argon using $CDCl_3$ or CD_2Cl_2 as solvents. ^1H and ^{13}C NMR spectra were measured on a JEOL FX90Q spectrometer operating at 89.6 MHz for ^1H. Some samples were also recorded by a JEOL GX270 spectrometer operating at 270.0 MHz. In each sample, concentration was adjusted in the range between 5 to 15 mM. Chemical shifts for Curie plots were read based on the internal TMS. The probe temperature was calibrated by the method of Van Geet [35]. Visible spectra were recorded on a Hitachi 200-10 spectrophotometer using CH_2Cl_2 as solvent. Samples for ESR measurement were dissolved in CH_2Cl_2 and were recorded on a JEOL FE2-XG X-band spectrometer operating with a 100 KHz field modulation of 6.3 gauss. The microwave frequency was monitored by an Advantest TR-5212 frequency counter. The magnetic field strength was calibrated by the hyperfine coupling constant of the Mn(II) ion doped in MgO powder (86.9 gauss).

3. Results and discussion

3.1. Low-temperature ^1H NMR spectra

^1H NMR spectra of the samples consisting of a high-spin (R-TPP)FeCl and 6.0 equiv. of a series of imidazole ligands L were taken at various temperatures. At −56 °C, each sample showed the formation of a low-spin complex, (R-TPP)Fe(L)$_2$Cl, at least partially except for one case; no formation of the low spin complex was observed in the sample consisting of (H-TPP)FeCl and 1-Me-2-^{i}PrIm. Pyrrole signals of the low-spin complexes can be classified into the following three categories according to their line shape: (a) no drastic change in signal shape even at −56 °C except for some broadening, (b) broadening of the signal followed by a split into four peaks, and (c) gradual appearance of four signals at lower temperatures.

Pyrrole signals of (H-TPP)Fe(L)$_2$Cl belong to category (a) regardless of the axial ligands. Pyrrole signals of (R-TPP)Fe(L)$_2$Cl also belong to this category, if L is an unhindered ligand such as HIm or 1-MeIm. As we have already reported, the split of the pyrrole signal in highly symmetrical (R-TPP)Fe(L)$_2$Cl is explainable only by the restricted rotation of the coordinated imidazole ligands [26]. Thus, the results indicate that even the rotation of hindered imidazoles is fast on the NMR time scale if the *meso* aryl groups have no substituents at the *o*-positions. The results also indicate that the rotation of unhindered imidazoles is fast even if bulky ^{i}Pr groups are introduced at the *o*-positions of *meso* aryl groups.

Pyrrole signals of (R-TPP)Fe(L)$_2$Cl, in which R is Me, Et or ^{i}Pr and L is a 2-alkylimidazole such as 2-MeIm, 2-EtIm, 2-^{i}PrIm or 1,2-Me_2Im, belong to category (b). Thus, the imidazoles in these complexes are fixed in a certain orientation at low temperature. In Fig. 1(a) the ^1H NMR spectrum of (^{i}Pr-TPP)Fe(2-MeIm)$_2$Cl taken at −45 °C is given as a typical example. One of the isopropyl methine signals corresponding to two protons appeared at −13.2 ppm, giving five peaks in total in the pyrrole signal region. In Fig. 1(b) the partially relaxed ^1H NMR spectrum of this complex obtained by an inversion–recovery pulse mode with a pulse interval of 50 ms is shown. While the *m*- and *p*-protons gave no signals under these conditions, the *o*-^{i}Pr methyl protons gave eight positive peaks due to their shorter relaxation times over a wide range of magnetic field, −3.5 to 7.0 ppm. These spectra suggest that the two methyl groups of each *o*-^{i}Pr group become diastereotopic when the rotation of the imidazole ligands

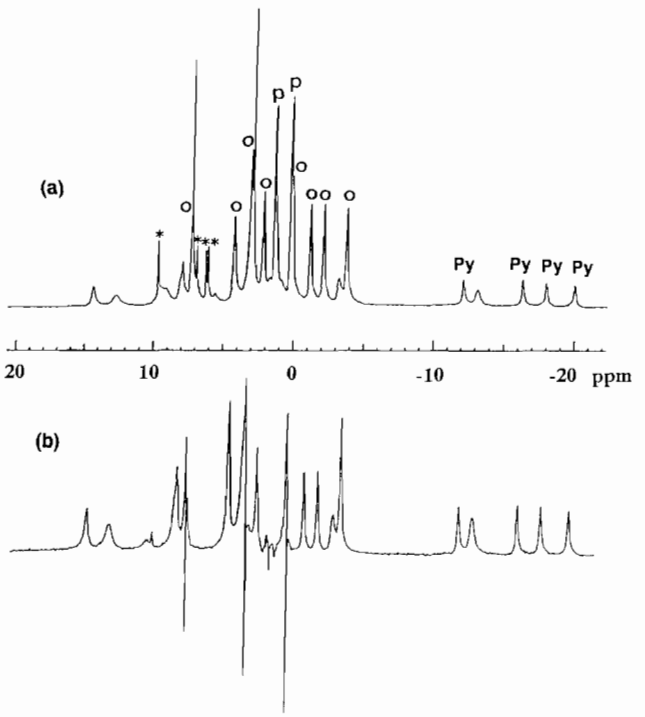

Fig. 1. (a) ^{1}H NMR spectrum of (^{i}Pr-TPP)Fe(2-MeIm)$_2$Cl in $CDCl_3$ at −45 °C. Assignment: o; *o*-methyl, p; *p*-methyl, py; pyrrole-H, *; *m*-H. (b) Partially relaxed ^{1}H NMR spectrum obtained by an inversion–recovery pulse mode with a pulse interval of 50 ms.

is slowed down. The pyrrole signals of the complexes with BzIm also belong to this category, although the temperature to give four signals is somewhat lower than those of the 2-alkylimidazoles; the broad pyrrole signal of (Me-TPP)Fe(BzIm)$_2$Cl at −56 °C split into four peaks at temperatures lower than −70 °C. The results suggest that the barriers to rotation of the 2-alkylimidazoles are higher than those of benzimidazole.

Pyrrole signals of the complexes with sterically very hindered 1-Me-2-^{i}PrIm belong to category (c). They showed no formation of the low-spin complex at ambient temperature. On lowering the temperature, the signal intensity of the high-spin complex decreased and four pyrrole signals due to the corresponding low-spin complex appeared. Even at −56 °C in the presence of 6 equiv. of the base, complete conversion into the low-spin complex could not be attained. The spectral behaviour can be explained in terms of the weak coordination ability of the 1-Me-2-^{i}PrIm ligand; the existence of the 1-methyl group would weaken the coordination ability of the ligand both due to its buttressing effect [36] and due to the lack of N–H···N hydrogen bonding [36–38]. This ligand can bind porphinatoiron(III) to form the low-spin complexes only when the *meso* aryl groups have *o*-substituents. In fact, no formation of the low-spin complex was observed in (H-TPP)FeCl even at −56 °C. Thus, the existence of *o*-alkyl substituents does not hinder the formation of low-spin bis(imidazole) complexes, in fact it stabilizes them in some cases [39,40]. A weak attractive interaction [41] between the ligands and *meso* substituents might be one of the reasons [42,43]. The chemical shifts of the pyrrole and *p*-Me signals at −56 °C together with the spread of the pyrrole shifts are listed in Table 1.

3.2. Orientation of coordinated ligands in solution

We have reported in a previous paper [26] that the 2-MeIm ligand in (Me-TPP)Fe(2-MeIm)$_2$Cl takes a mutually perpendicular alignment over the diagonal N–Fe–N axes. We reached this conclusion based on the splitting pattern of the ^{1}H NMR signals at low temperatures where rotation of the ligands slowed down on the NMR time scale; four peaks of *o*-Me, *m*-H and pyrrole-H are suggestive of the orientation shown in **A** or **B** of Fig. 2. Although the number of *p*-Me signals, two peaks with equal intensity, supported conformer **A**, we preferred conformer **B** for the following two reasons: (i) the chemical shifts may accidentally coincide since the *p*-Me protons are located far away from the paramagnetic center, (ii) the 2-Me of imidazole would interact repulsively with the *o*-Me of the mesityl group in conformer **A**. However, in the present study using a series of (R-TPP)Fe(L)$_2$Cl, the *p*-alkyl signals always split into two signals with equal intensity as shown in Table 1. The results suggest that the stable conformation of these complexes is **A** in which two imidazole rings are placed over diagonal C_{meso}–Fe–C_{meso} axes.

Temperature-dependent ^{13}C NMR spectra of ^{13}C (99% ^{13}C) enriched (Me-TPP)Fe(2-MeIm)$_2$Cl at the four *meso* positions would give solid evidence on the conformation of these complexes. If **A** is the stable conformer, two signals with equal intensity would be observed. On the contrary, conformer **B** should give three signals in a 1:2:1 intensity ratio. Fig. 3(a) shows the temperature dependent ^{13}C NMR spectra. Corresponding to the ^{1}H NMR result, the single peak at 129 ppm at 32 °C broadened on lowering the temperature and split into two peaks of equal integral intensity below −25 °C. Although the peak at higher magnetic field is broader than the other, further lowering of the temperature by using a high field spectrometer gave two signals with equal intensity as shown in Fig. 3(b). Since the accidental coincidence of the two signals is highly improbable in the case of *meso* carbons due to their close location to the paramagnetic center, it is clear that the stable conformation of these complexes should be given by **A** [40]. The same conclusion was obtained by Walker and Simonis based on the 2D NOESY spectroscopic technique [44].

The question arises as to why conformer **A**, where a large repulsive interaction is expected between the 2-alkyl group of imidazole and the *o*-alkyl group of porphyrin, is more stable than conformer **B**. Recent

Table 1
Chemical shifts of the pyrrole and *p*-methyl protons in (R-TPP)Fe(L)$_2$Cl at −56 °C (90 MHz, $CDCl_3$)

R	L	Pyrrole shifts (spread)					*p*-Methyl	
Me	2-MeIm	−14.7	−19.0	−21.0	−23.3	(8.6)	1.2	2.2
Me	2-EtIm	−12.7	−17.7	−19.6	−22.8	(10.1)	1.2	2.7
Me	2-^{i}PrIm	−12.9	−18.8	−20.6	−23.6	(10.7)	1.2	2.6
Me	2-^{i}PrIm, 1-MeIm[a]	−13.7	−17.0	−25.3	−30.8	(17.1)	1.0	1.6
Me	1,2-Me$_2$Im	−9.8	−14.3	−15.9	−19.1	(9.3)	1.4	2.9
Me	1-Me-2-^{i}PrIm	−6.7	−12.5	−14.1	−17.9	(11.2)	1.5	3.0
Me	BzIm[b]	−13.5	−15.9	−18.4	−21.3	(7.8)	1.1	2.4
Et	2-MeIm	−15.1	−19.9	−21.7	−24.2	(9.1)	0.0	1.0
Et	2-EtIm	−15.0	−20.0	−21.9	−24.9	(9.9)	0.1	1.3
Et	2-^{i}PrIm	−14.6	−20.4	−22.1	−25.7	(11.1)	0.1	1.4
Et	2-^{i}PrIm, 1-MeIm	−13.8	−18.1	−27.9	−33.2	(19.4)		[c]
Et	1,2-Me$_2$Im	−13.2	−18.9	−20.3	−23.5	(10.3)	0.1	1.4
Et	1-Me-2-^{i}PrIm	−7.8	−13.6	−15.3	−19.7	(11.9)	0.4	1.8
Et	BzIm[d]	−15.8	−20.5	−22.8	−27.2	(11.4)	−0.4	1.2
^{i}Pr	2-MeIm	−13.0	−17.6	−19.4	−21.5	(8.5)	0.1	1.3
^{i}Pr	2-EtIm	−14.0	−19.7	−21.2	−24.4	(10.4)	0.2	1.2
^{i}Pr	2-^{i}PrIm	−12.2	−17.6	−19.1	−22.3	(10.1)	0.3	1.6
^{i}Pr	2-^{i}PrIm, 1-MeIm	−15.0	−16.5	−31.5	−33.0	(18.0)		[c]
^{i}Pr	1,2-Me$_2$Im	−10.9	−16.4	−17.6	−20.6	(9.7)	0.1	1.3
^{i}Pr	1-Me-2-^{i}PrIm	−7.8	−13.7	−15.3	−19.5	(11.7)	0.5	1.8
^{i}Pr	BzIm	−11.8	−15.9	−18.1	−22.3	(10.5)	0.0	1.2

[a]Chemical shifts of two of the three *p*-methyl signals are given.
[b]Chemical shifts at −79 °C in $CD_2Cl_2/CDCl_3$ (1:1).
[c]*p*-Methyl signals were difficult to assign.
[d]Chemical shifts at −73 °C in $CD_2Cl_2/CDCl_3$ (1:1).

X-ray crystallographic studies on (H-TPP)Fe(2-MeIm)$_2$$ClO_4$ [45], (H-TPP)Fe(Py)$_2$$ClO_4$·2THF [17] and (Me-TPP)Fe(4-NMe_2Py)$_2$$ClO_4$ [46], where Py and 4-NMe_2Py are pyridine and 4-(*N*,*N*-dimethylamino)-pyridine, respectively, suggested that the porphinatoiron core of these complexes is not planar, but instead shows a substantial S_4 ruffled structure. The axial ligands in these complexes are placed in the cavities along two diagonal C_{meso}–Fe–C_{meso} axes created by the deformed porphinatoiron core with a right angle to each other, thus minimizing the repulsion between core and ligand [44]. In solution, the deformed porphyrin core is expected to show fluxional behavior interconverting from one S_4 structure to another [47]. If the axial ligands are hindered imidazoles, the S_4 deformed structure would be tightly fixed. Thus, the rate of rotation is expected to become smaller. Further discussion on this is given later in this paper.

The deformed porphyrin core mentioned above has the C_2 axis along the diagonal N–Fe–N. Thus, the two isopropyl methyl groups of the coordinated 2-^{i}PrIm in (Me-TPP)Fe(2-^{i}PrIm)$_2$Cl become diastereotopic if rotation of the ligands is hindered and the two imidazoles are fixed perpendicularly. The ^{1}H NMR spectrum of this complex at −1.2 °C is given in Fig. 4. Assignment of the isopropyl methyl groups of the coordinated 2-^{i}PrIm was achieved by the saturation transfer experiment [40,48–50]. Fig. 4(b) shows the spectrum obtained by the irradiation of the isopropyl methyl signals of free 2-^{i}PrIm at 1.7 ppm. The intensity of the signals at −6.2 and 0.2 ppm decreased to a great extent. Correspondingly, irradiation of the signal at −6.2 ppm decreased the intensity of the signals at 0.2 and 1.7 ppm as shown in Fig. 4(c). The same experiment at −30 °C, however, did not cause any appreciable effect on their intensity, indicating that the signals at 0.2 and −6.2 ppm are exchanging with the signal at 1.7 ppm. Thus, the observed peaks at 0.2 and −6.2 ppm at −1.2 °C are assigned to the isopropyl methyl groups of the coordinated 2-^{i}PrIm. These signals moved to −0.1 and −9.8 ppm, respectively, at −56 °C. (Et-TPP)Fe(2-^{i}PrIm)$_2$Cl and (^{i}Pr-TPP)Fe(2-^{i}PrIm)$_2$Cl also exhibited two signals for the isopropyl methyls; the former showed the signals at −1.1 and −9.2 and the latter at −0.5 and −10.1 ppm at −56 °C.

3.3. Spread of pyrrole shifts

The data in Table 1 indicate that the spread of the pyrrole signals of (R-TPP)Fe(L)$_2$Cl is in the range 8.6–11.9 ppm at −56 °C. If the porphyrin core is planar and the axial ligands are placed perpendicularly to each other, both of the d_π orbitals of iron equally interact with the π orbitals of the imidazole rings. Consequently,

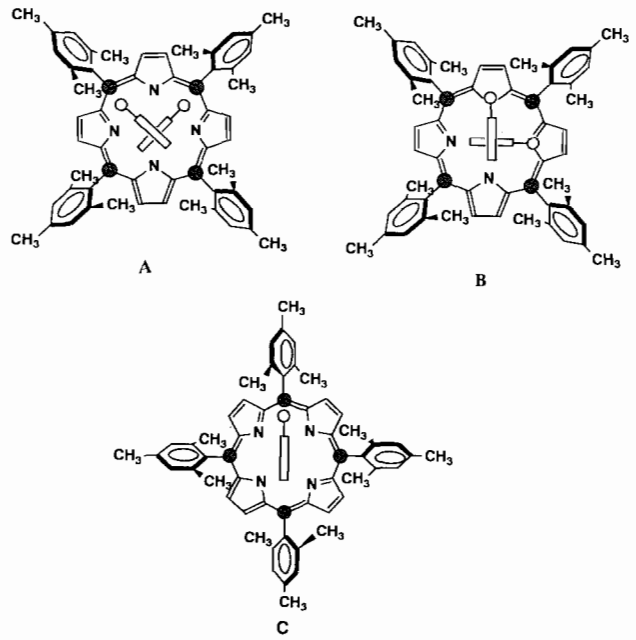

Fig. 2. Possible orientation of the axial ligands. Black circles indicate the positions where carbons are enriched by ^{13}C. **A**: two axial ligands are placed perpendicularly along the diagonal C_{meso}–Fe–C_{meso} axes, giving two *meso* signals of equal intensity. **B**: two axial ligands are placed perpendicularly along the diagonal N–Fe–N axes, giving three *meso* signals of 1:2:1 intensity ratio. **C**: one of the axial ligands is fixed along the diagonal C_{meso}–Fe–C_{meso} axis, while the other ligand is rapidly rotating, giving three signals of 1:2:1 ratio.

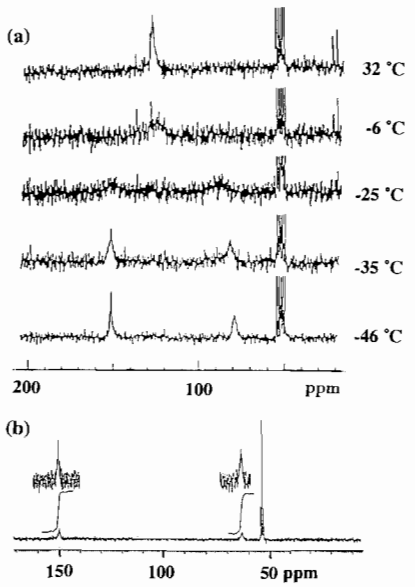

Fig. 3. (a) Temperature-dependent ^{13}C NMR spectra of *meso* ^{13}C enriched (Me-TPP)Fe(2-MeIm)$_2$Cl in CD_2Cl_2 measured on a 22.5 MHz spectrometer. (b) ^{13}C NMR spectrum at −71 °C measured on a 67.5 MHz spectrometer.

an unpaired electron resides in both the d_π orbitals and is transferred equally to the eight pyrrole carbons. Thus, the eight pyrrole protons should show similar

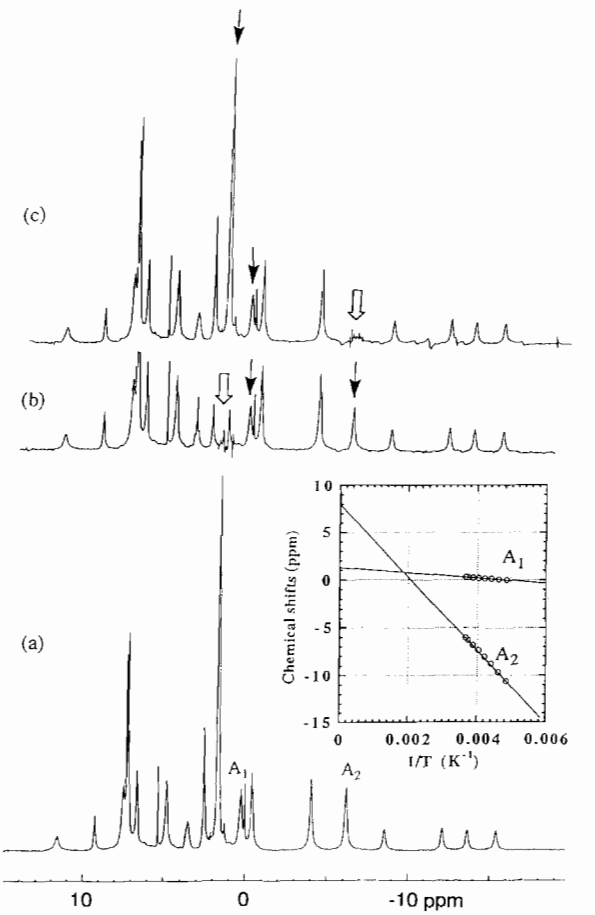

Fig. 4. (a) ^1H NMR spectra of (Me-TPP)Fe(2-^{i}PrIm)$_2$Cl taken at −1.2 °C. A_1 and A_2 are the isopropyl methyls of the coordinated 2-^{i}PrIm. (b) Change in signal intensity when the isopropyl methyl signals of free 2-^{i}PrIm, $\delta = 1.7$ ppm, were irradiated. (c) Change in signal intensity when the signal at $\delta = -6.2$ ppm, A_2, was irradiated. Inset: temperature dependence of the isopropyl methyl signals, A_1 and A_2, of the coordinated 2-^{i}PrIm; A_1: $\delta = -258/T + 1.25$, A_2: $\delta = -3850/T + 8.08$.

chemical shifts. A relatively large spread of the pyrrole shifts might be ascribed to the non-planar nature of the porphinatoiron core.

It would be interesting to compare the ^1H NMR spectra of the complexes mentioned above with those of the complexes carrying two parallel fixed ligands. It is very difficult, however, to obtain such complexes because the introduction of an alkyl group at the 2-position of imidazole to freeze its rotation necessarily causes S_4 deviation of the porphinatoiron core and makes the two ligands align perpendicularly. A complex in which one of the axial ligands is fixed and the other is rapidly rotating could be a substitute, since the orientation effect of a rapidly rotating ligand is, to some extent, canceled out. Although the mixed ligand complexes, (Me-TPP)Fe(2-MeIm)(1MeIm)Cl and (Me-TPP)Fe(2-MeIm)(CN), showed no split of the pyrrole

signals even at −88 °C due to their low barriers to rotation [27], (Me-TPP)Fe(2-^{i}PrIm)(1-MeIm)Cl exhibited a split below −45 °C [51]. This complex was formed by the addition of 1-MeIm (4.3 equiv.) and 2-^{i}PrIm (3.0 equiv.) into a $CDCl_3$ solution containing (Me-TPP)FeCl. Fig. 5 shows the temperature-dependent ^{1}H NMR spectrum of this sample. Signals signified as X, Y and Z correspond to the pyrrole protons of bis(2-^{i}PrIm), mixed ligand and bis(1-MeIm) complexes, respectively. The pyrrole protons of the mixed ligand complex gave a sharp singlet at room temperature, which broadened and split into four peaks, −13.7, −17.0, −25.3 and −30.8 ppm, at −56 °C. Thus, the spread of the signals reached 17.1 ppm, nearly twice as much as that of (Me-TPP)Fe(2-MeIm)$_2$Cl. Similarly, (Et-TPP)Fe(2-^{i}PrIm)(1-MeIm)Cl and (^{i}Pr-TPP)Fe(2-^{i}PrIm)(1-MeIm)Cl exhibited large spreads of the pyrrole signals, 19.4 and 18.0, respectively, as listed in Table 1. The fact that the pyrrole protons split into four signals in the mixed ligand complex suggests that the rotation of only one of the axial ligands, 2-^{i}PrIm, slowed down at low temperature; hindered rotation of both ligands should give eight pyrrole signals. In contrast to the case of (Me-TPP)Fe(2-^{i}PrIm)$_2$Cl, the isopropyl methyl protons of the mixed ligand complex gave a single peak even at −56 °C. The result is further evidence that the rotation of only one of the axial ligands, 2-^{i}PrIm, is frozen; the slow rotation of 1-MeIm makes the two isopropyl methyl groups diastereotopic, giving two signals as in the case of (Me-TPP)Fe(2-^{i}PrIm)$_2$Cl [1]. The temperature dependence of the coordinated isopropyl methyl signal is given in the inset of Fig. 5. The slope of the line was −1340 ppm/K, just between the slopes of the A_1 (−258 ppm/K) and A_2 (−3850 ppm/K) lines of (Me-TPP)Fe(2-^{i}PrIm)$_2$Cl.

Orientation of the fixed ligand in (Me-TPP)Fe(2-^{i}PrIm)(1-MeIm)Cl relative to the porphyrin ring was examined by ^{13}C NMR spectroscopy. A $CDCl_3$ solution of ^{13}C (99% ^{13}C) enriched (Me-TPP)Fe(2-^{i}PrIm)$_2$Cl at the four *meso* positions was titrated with 1-MeIm and the subsequent spectral change was monitored at −56 °C. As the amount of added 1-MeIm increased, the *meso* signals of the starting bis(2-^{i}PrIm) at δ 81 and 163 ppm decreased and three new signals of the mixed ligand complex centered at δ 44, 92 and 106 ppm appeared in a 1:2:1 intensity ratio. On further addition of 1-MeIm, the intensity of the signal of bis(1-MeIm) at δ 36 ppm became a major peak. The result clearly suggests that the 2-^{i}PrIm ligand is fixed along the diagonal C_{meso}–Fe–C_{meso} axis as shown in **C** of Fig. 2; fixation of 2-^{i}PrIm along the diagonal N–Fe–N axis should give two signals of equal intensity.

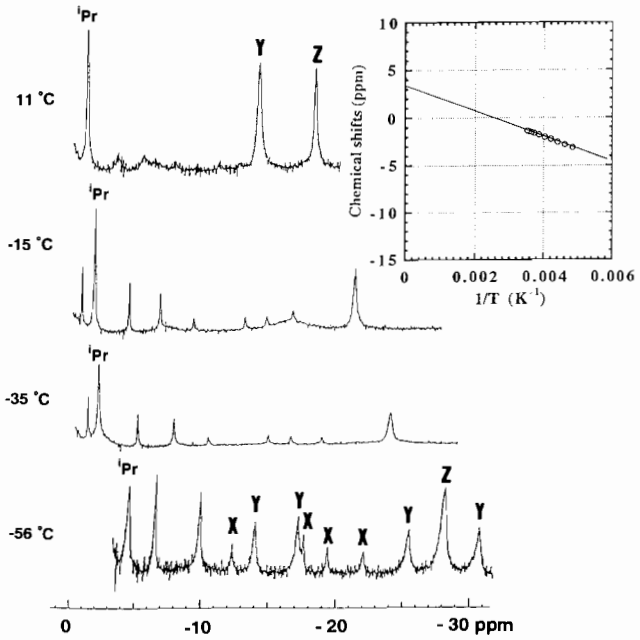

Fig. 5. Temperature-dependent ^{1}H NMR spectra of a sample consisting of (Me-TPP)FeCl (1.0 equiv.), 1-MeIm (3.0 equiv.) and 2-^{i}PrIm (4.3 equiv.). Only a high field region is given. X, Y and Z are the pyrrole signals of (Me-TPP)Fe(2-^{i}PrIm)$_2$Cl, (Me-TPP)Fe(2-^{i}PrIm)(Me-TPP)Cl and (Me-TPP)Fe(1-MeIm)$_2$Cl, respectively. ^{i}Pr is the methyl signal of the coordinated 2-^{i}PrIm in the mixed ligand complex. Inset: temperature dependence of the isopropyl methyl signal of the mixed ligand complex; $\delta = -1340/T + 3.38$.

3.4. Curie plots

Chemical shifts of the pyrrole signals of a series of low-spin complexes were plotted against $1/T$. For the complexes showing four pyrrole signals at low temperatures, the average position of the four peaks was taken as the chemical shift. In principle, axial and rhombic terms of the dipolar contribution toward pyrrole chemical shifts should be different depending upon the temperature, since the population of conformers is also temperature dependent. In the present system, however, conformer **A** in Fig. 2 is expected to be the only species in solution throughout the temperature range examined; other conformers such as **B** in Fig. 2 and parallel conformers are supposed to be quite unstable. In fact, the plot gave a reasonably good straight line in a wide temperature range, typically between 30 and −65 °C. Deviation from linearity was observed, however, at higher temperatures where the high-spin complex starts to appear. Those data were excluded in data processing. In the case of (R-TPP)Fe(1-Me-2-^{i}PrIm)$_2$Cl, the low-spin complex appeared only below −20 °C and the starting high-spin complex remained even at −75 °C.

[1] We cannot completely rule out the possibility at this point that the rotation of 1-MeIm in the mixed ligand complex, (^{i}Pr-TPP)Fe(2-^{i}PrIm)(1-MeIm)Cl, is also hindered. As one of the referees pointed out, it might be possible that the fixed 1-MeIm cannot create observable non-equivalence in the pyrrole protons or in the isopropyl methyl protons because of the great distance of these protons from the axial ligand.

In these complexes, the average positions of the four pyrrole peaks were taken as the chemical shifts, in spite of the presence of the high-spin complex. The slopes and intercepts thus obtained are listed in Table 2. The data in Table 2 clearly indicate that the complexes with rapidly rotating imidazole ligands such as (H-TPP)Fe(L)$_2$Cl (L is both hindered and unhindered imidazole), (R-TPP)Fe(HIm)$_2$Cl and (R-TPP)Fe(1-MeIm)$_2$Cl have larger negative slopes; the absolute values for the slopes of the 13 complexes with rapidly rotating axial ligands were in the small region of 8370 ± 370 ppm/K. The only exception was (^{i}Pr-TPP)Fe(HIm)$_2$Cl which showed a smaller value for the slope, 7250 ppm/K. On the other hand, the average slope of the 18 complexes with slowly rotating axial ligands was 5270 ppm/K. As a result, the average chemical shift of the pyrrole protons at -56 °C was -25.3 ppm for the former complexes in contrast to -16.5 ppm for the latter ones. The data in Table 2 also revealed that the complexes with 1,2-disubstituted imidazoles have smaller absolute values than those with 2-alkylimidazoles and benzimidazole. The average slope for the 6 complexes with 1,2-disubstituted imidazoles was 4360 ppm/K, while that for the 12 complexes with 2-alkylimidazoles and benzimidazole was 5700 ppm/K. In an extreme case, the slope and the chemical shift of (Me-TPP)Fe(1-Me-2-^{i}PrIm)$_2$Cl were 3880 ppm/K and -12.8 ppm, respectively, at -56 °C.

One of the factors affecting the chemical shifts of the pyrrole protons in low-spin ferric porphyrin complexes is the basicity of axial ligands. As La Mar and Walker [52] reported, the pyrrole signals of a series of (H-TPP)Fe(4-X-Py)$_2$I appeared over a range of 22 ppm at -60 °C depending upon the basicity of the 4-substituted pyridine (4-X-Py); the isotropic shifts of the pyrrole protons increase as the basicity of the axial ligand becomes stronger. A much stronger dependence on basicity was reported by Safo et al. [53] in (Me-TPP)Fe(X-Py)ClO$_4$, where the pyrrole shifts spanned a range of about 33 ppm at -80 °C. In the present

Table 2
Slopes and intercepts of the Curie plots and the average chemical shifts of the pyrrole protons in (R-TPP)Fe(L)$_2$Cl at -56 °C

R	L	Slopes ($\times 10^{-3}$ ppm·K)	Intercepts (ppm)	Chemical shifts (ppm, -56 °C)
H	HIm	-8.58	12.0	-27.4
H	1-MeIm	-8.68	11.9	-27.9
H	2-MeIm	-8.56	16.0	-23.3
H	2-EtIm	-8.74	17.8	-22.3
H	2-^{i}PrIm	-8.00	14.9	-21.8
H	1,2-Me$_2$Im	-8.67	18.4	-21.4
H	1-Me-2-^{i}PrIm[a]			
H	BzIm	-8.55	16.9	-22.3
Me	HIm	-8.31	11.1	-27.0
Me	1-MeIm	-8.62	11.8	-27.7
Me	2-MeIm	-6.01	9.4	-18.2
Me	2-EtIm	-5.68	9.3	-16.8
Me	2-^{i}PrIm	-5.53	7.8	-17.6
Me	1,2-Me$_2$Im	-4.53	7.2	-13.6
Me	1-Me-2-^{i}PrIm	-3.88	5.1	-12.8
Me	BzIm	-5.25	7.4	-16.7
Et	HIm	-8.37	11.0	-27.4
Et	1-MeIm	-8.65	11.6	-28.1
Et	2-MeIm	-5.97	8.7	-18.7
Et	2-EtIm	-6.40	10.4	-19.0
Et	2-^{i}PrIm	-6.12	9.0	-19.1
Et	1,2-Me$_2$Im	-5.37	8.3	-16.3
Et	1-Me-2-^{i}PrIm	-4.19	5.2	-14.0
Et	BzIm	-5.93	9.0	-18.2
^{i}Pr	HIm	-7.25	7.8	-25.5
^{i}Pr	1-MeIm	-8.05	9.9	-27.0
^{i}Pr	2-MeIm	-5.47	7.5	-17.6
^{i}Pr	2-EtIm	-5.74	8.1	-18.2
^{i}Pr	2-^{i}PrIm	-5.12	6.2	-14.0
^{i}Pr	1,2-Me$_2$Im	-4.55	5.7	-15.2
^{i}Pr	1-Me-2-^{i}PrIm	-4.15	5.0	-13.9
^{i}Pr	BzIm	-5.22	7.0	-16.9

[a]Low-spin complex was not formed even at -56 °C.

system, however, basicity of the ligands showed little correlation with the chemical shifts; while 2-EtIm ($pK_b = 6.0$) is stronger as a base than HIm ($pK_b = 7.0$) and 1-MeIm ($pK_b = 6.7$) [54], the isotropic shift of the pyrrole protons in (R-TPP)Fe(2-EtIm)$_2$Cl is much smaller than those of the corresponding bis(Him) and bis(1-MeIm) complexes. Thus, the large differences in the pyrrole shifts and Curie slopes must be ascribed to steric effects caused by the repulsion between the axial ligands and porphinatoiron core. The data in Table 2 suggest that the unpaired electron of iron is transferred more effectively to the porphyrin ring in the complexes with unhindered imidazoles than in the complexes with hindered ones. This is understandable since one of the factors controlling the spin transfer is the effective overlap of the porphyrin p_π and iron d_π orbitals [55], which is supposed to be much larger in the complexes with rapidly rotating ligands due to their planarity; although the degree of non-planarity of the complexes such as (R-TPP)Fe(2-MeIm)$_2^+$ is not known due to the lack of X-ray crystallographic studies, the complex with hindered imidazole, (H-TPP)Fe(2-MeIm)$_2$ClO$_4$ [45], showed a much deeper S_4-ruffled structure than the complexes with unhindered imidazole such as (H-TPP)Fe(HIm)$_2$Cl [56] and (H-TPP)Fe(1-MeIm)$_2$ClO$_4$ [57]. Thus, the slopes of Curie plots in low-spin bis(alkylimidazole) complexes could be a good probe to elucidate how much the porphinatoiron core deviates from planarity.

The slopes and intercepts of the *meso* ^{13}C signals of some low-spin complexes are listed in Table 3 together with the chemical shifts at −56 °C. As in the case of the pyrrole-H signals, the absolute values of the Curie slopes of the H-TPP complexes were larger than those of the corresponding Me-TPP complexes with hindered axial ligands. The data in Table 3 also indicate that the isotropic shifts of (Me-TPP)Fe(2-MeIm)$_2$Cl and (Me-TPP)Fe(BzIm)$_2$Cl, calculated based on the *meso* ^{13}C shift of the analogous diamagnetic (H-TPP)Co(HIm)$_2$Cl [58], are only +6 and −8 ppm at −56 °C, respectively, as compared with +56 and +44 ppm of the corresponding H-TPP complexes. These results suggest that the spin transfer to the *meso* carbons of Me-TPP complexes with hindered axial ligands is smaller than that of the corresponding H-TPP complexes.

Table 3
Slopes and intercepts of the Curie plots and the average chemical shifts of the *meso* ^{13}C signals in some (R-TPP)Fe(L)$_2$Cl at −56 °C

R	L	Slopes ($\times 10^{-3}$ ppm·K)	Intercepts (ppm)	Chemical shifts[a] (ppm, −56 °C)
H	1-MeIm	−25.0	143	27.3
H	2-MeIm	−26.1	184	63.7
H	BzIm	−19.9	168	75.9
Me	1-MeIm	−24.2	148	36.9
Me	2-MeIm	−10.6	162	114
Me	BzIm	−5.5	153	128

[a]Chemical shift of a diamagnetic (H-TPP)Co(HIm)$_2$Cl is reported to be 119.9 ppm [58].

3.5. Barriers to rotation of imidazole ligands

Barriers to rotation [50,59] of the coordinated imidazoles were determined based on the change in line shape of the *p*-alkyl signals. In some cases, these signals were hidden by the 2-alkyl signals of the added excess imidazoles, making it difficult to perform the computer simulation. Thus, the barriers to rotation were estimated by the coalescence temperature method. In Table 4 are listed the activation free energies for rotation together with the coalescence temperatures.

Before discussing the data in Table 4, mechanisms for the dynamic process which cause the change in line shape of the *p*-alkyl signals have to be considered. As shown in Fig. 6, two types of dynamic process can explain the observed spectral change. Process (a) is a pure rotation about the Fe–N_{axial} bond and process (b) is a dissociation–association of the axial ligands. The pure rotation process is observable only when the barriers to ligand dissociation are considerably larger than those for the pure rotation. A convenient way to discriminate (a) from (b) is to irradiate the alkyl signal of the free imidazole at the temperature where the *p*-alkyl signals start to exhibit exchange broadening. If the intensity of the alkyl signals of the coordinated imidazole shows no change, the process is assigned to a pure rotation. In contrast, if the intensity decreases

Table 4
Activation free energies for the dynamic process corresponding to the change in line shape of the *p*-methyl signals in (R-TPP)Fe(L)$_2$Cl together with coalescence temperatures

R	L	T_c (°C)	ΔG_c^* (kcal mol^{-1})	Mechanism[a]
Me	2-MeIm	−22.0	12.0	R
Me	2-EtIm	−7.5	12.5	R
Me	2-^{i}PrIm	14.0	13.6	R, D
Me	1,2-Me$_2$Im	−34.4	11.3	R
Me	BzIm	−69.6	9.8	R
Et	2-MeIm	−10.6	12.7	R
Et	2-EtIm	−3.3	12.8	R
Et	2-^{i}PrIm	11.0	13.6	R, D
Et	1,2-Me$_2$Im	−25.1	11.9	R
Et	BzIm	−58.2	10.2	R
^{i}Pr	2-MeIm	−4.4	12.9	R
^{i}Pr	2-EtIm	11.0	13.6	R
^{i}Pr	2-^{i}PrIm	11.3	13.6	R, D
^{i}Pr	1,2-Me$_2$Im	−19.9	12.4	R
^{i}Pr	BzIm	−30.3	11.8	R

[a]Mechanism for ligand exchange; R: rotation, D: dissociation–reassociation.

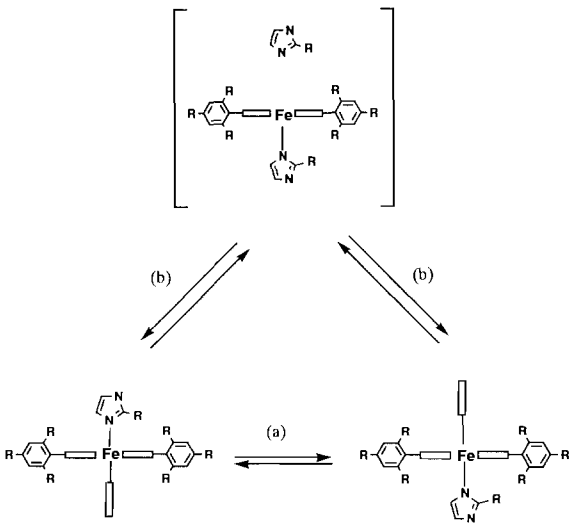

Fig. 6. The two types of dynamic process: (a) pure rotation process, (b) dissociation–association process.

due to saturation transfer between free and coordinated ligands, the dissociation–association process is involved at least partially. An irradiation experiment has revealed that process (b) is involved in the case of (R-TPP)Fe(2-^{i}PrIm)$_2$Cl. In other complexes, however, rotation of the ligands was the only dynamic process responsible for the temperature-dependent spectra at low temperature.

The data in Table 4 indicate that the barriers to rotation of 2-MeIm increase as the *o*-substituents change from Me, Et, and then to the ^{i}Pr group. The same is true for 2-EtIm, 2-^{i}PrIm, 1,2-Me$_2$Im and BzIm. Similarly, barriers to rotation increase in a series of porphyrins when the axial ligand changes from BzIm, 1,2-Me$_2$Im, 2-MeIm, 2-EtIm, and then to 2-^{i}PrIm. It is noteworthy that the activation free energies of 2-^{i}PrIm are nearly the same regardless of the kind of *o*-substituent, 13.6 kcal mol^{-1}. The result suggests that ligand dissociation takes place at similar temperatures. Thus, the real barriers to rotation of 2-^{i}PrIm must be higher than 13.6 kcal mol^{-1}.

When one of the hindered ligands is replaced by an unhindered ligand as in the case of (Me-TPP)Fe(2-MeIm)(1-MeIm)Cl, the rotational barrier of 2-MeIm greatly decreased; the activation free energy changed from 12.0 kcal mol^{-1} (−22 °C) in (Me-TPP)Fe(2-MeIm)$_2$Cl to less than 8.8 kcal mol^{-1} (−88 °C) in (Me-TPP)Fe(2-MeIm)(1-MeIm)Cl and (Me-TPP)Fe(2-MeIm)(CN) [27]. The large decrease in activation free energies of the 2-MeIm ligand can be explained as follows. As the 2-MeIm rotates from its most stable site, the porphinatoiron core ruffles concomitantly to minimize the steric repulsion. The structural change of the core might be much easier in the complexes with unhindered ligand at the 6th position than in the complexes with two hindered ligands, since the S_4 deformed structure is tightly fixed when both of the axial ligands are hindered imidazoles. Thus, the rotational barrier of the 2-MeIm ligand in the mixed ligand complex becomes much smaller than that of the corresponding bis(2-MeIm) complex. As mentioned, fixation of one of the ligands was achieved in (Me-TPP)Fe(2-^{i}PrIm)(1-MeIm)Cl. Two sharp signals of the *p*-methyls were observed at 1.0 and 1.6 ppm at −56 °C with an intensity ratio of about 2:1, though the other signal expected from conformer **C** (Fig. 2) was not detected due to the presence of intense isopropyl methyl signals of the free ligand. The coalescence temperature of the *p*-methyl signals was not determined precisely, but it was in the temperature range between −35 and −45 °C. Thus, the difference in coalescence temperatures between (Me-TPP)Fe(2-^{i}PrIm)$_2$Cl and (Me-TPP)Fe(2-^{i}PrIm)(1-MeIm)Cl is estimated to be ~55 °C.

Complexes with BzIm as axial ligands have smaller barriers to rotation than those of the corresponding bis(2-alkylimidazole) complexes; the differences in activation free energies between (R-TPP)Fe(2-MeIm)$_2$Cl and (R-TPP)Fe(BzIm)$_2$Cl were 2.2, 2.5, and 1.1 kcal mol^{-1} for R = Me, Et and ^{i}Pr, respectively. The easier rotation of the BzIm ligands in bis(BzIm) was ascribed to the increase in energy level of the ground state of rotation due to the severe steric repulsion between 4-H of the benzimidazole ring and the porphinatoiron core.

3.6. ESR spectra

X-band ESR spectra of some low-spin complexes were measured at 4.2 K in CH_2Cl_2 glass. The *g* values of these complexes are listed in Table 5. As typical examples, the ESR spectra of (Me-TPP)Fe(HIm)$_2$Cl, (Me-TPP)Fe(2-MeIm)$_2$Cl and (Me-TPP)Fe(BzIm)$_2$Cl are given in Fig. 7. The data in Table 5 indicate that (R-TPP)Fe(HIm)$_2$Cl gave characteristic rhombic signals at $g_z = 2.9$–3.0, $g_y = 2.3$–2.4 and $g_x = 1.2$–1.6. In contrast, (R-TPP)Fe(2-MeIm)$_2$Cl complexes gave broad signals with large g_z values, $g_z = 3.1$–3.2. In these complexes, signals corresponding to g_x were not observable. Walker et al. [16,53] reported that the complexes with parallel aligned ligands usually give rhombic signals, while those with perpendicular aligned ligands exhibit so called 'strong g_{max}' type signals; the signal with $g_{max} > 3.1$ as the sole observable spectral feature. Although the orientation of the HIm ligand in (R-TPP)Fe(HIm)$_2$Cl in solution could not be determined by the NMR method presented here due to its fast rotation, a crystallographic study of the analogous (H-TPP)Fe(HIm)$_2$ClO$_4$ showed a parallel alignment of the ligand [57].

The large ESR g_z values in (R-TPP)Fe(2-MeIm)$_2$Cl are consistent with the low-temperature NMR results showing that the axial ligands of these complexes take a perpendicular alignment. Close examination of the

Table 5
ESR parameters of (R-TPP)Fe(L)$_2$Cl in CH_2Cl_2 at 4.2 K

	g_z	g_y	g_x
(R-TPP)Fe(HIm)$_2$Cl			
R = H[a]	2.87	2.29	1.56
R = Me	2.92	2.29	1.57
R = Et	3.05	2.28	1.22
R = ^{i}Pr	2.95	2.37	1.29
(R-TPP)Fe(2-MeIm)$_2$Cl			
R = H[a]	3.40	1.74	1.19
R = Me	3.13	1.9	[c]
R = Et	3.17	1.9	[c]
R = ^{i}Pr	3.08	1.9	[c]
(R-TPP)Fe(BzIm)$_2$Cl			
R = H[b]	3.43	1.67	1.19
R = Me	2.89	2.29	[c]
R = Et	2.93	2.29	[c]
R = ^{i}Pr	3.01	2.21	[c]

[a]Ref. [10].
[b]Values for (H-TPP)Fe(5,6-Me$_2$BzIm)$_2^+$ quoted from Ref. [10].
[c]The linewidth for the g_x component was too broad to estimate an accurate g value.

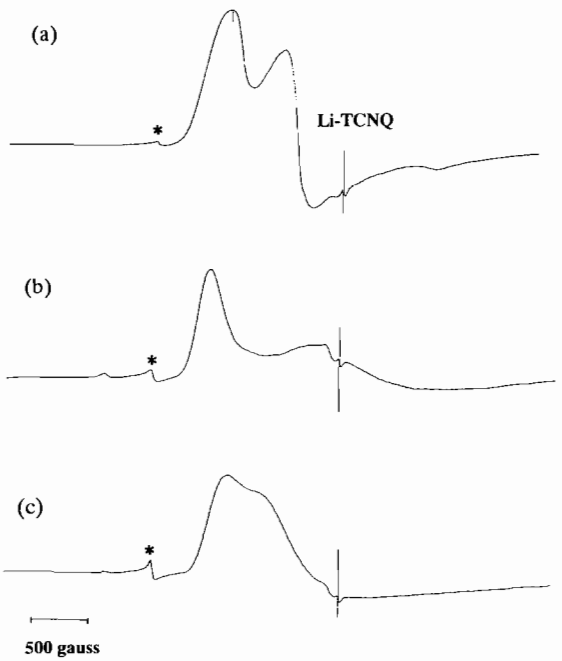

Fig. 7. ESR spectra of some low-spin (Me-TPP)Fe(L)$_2$Cl in CH_2Cl_2 glass at 4.2 K. The weak ESR signal signified by * at $g = 4.3$ would be assigned to a non-heme iron complex. (a) L = HIm, (b) L = 2-MeIm, (c) L = BzIm.

data in Table 5, however, reveals that the g_z values decrease when the alkyl groups are introduced to the *o*-position of the *meso* aryl groups; while the g_z value of (H-TPP)Fe(2-MeIm)$_2$Cl is 3.40 [10], those of (R-TPP)Fe(2-MeIm)$_2$Cl are 3.13 [40][2], 3.17 and 3.08 for the complexes with R = Me, Et and ^{i}Pr, respectively. The difference in g_z values between *o*-substituted and *o*-unsubstituted complexes is exemplified much clearer in the case of bis(BzIm) complexes; while the g_z value of (H-TPP)Fe(5,6-Me$_2$BzIm)$_2$Cl is 3.43 [10], those of (R-TPP)Fe(BzIm)$_2$Cl are in the range 2.89–3.01. The results suggest that the perpendicular alignment is not the only reason for the large g_z value, consistent with the results obtained by Safo et al. [53]. It is not clear why the complexes with sterically hindered imidazole ligands show ESR spectra with smaller g_z values. The difference in planarity of the porphyrin ring between (H-TPP)Fe(BzIm)$_2$Cl and (R-TPP)Fe(BzIm)$_2$Cl must be one of the reasons. Further work on the relationship between the planarity of the porphyrin and the ESR spectral properties is in progress.

[2]Safo et al. reported the g value of (Me-TPP)Fe(2-MeIm)$_2$ClO$_4$ to be 3.17 in the solid state [53].

Acknowledgements

This work was partly supported by a Grant in Aid for Scientific Research (No. 05640617) from Ministry of Education, Science and Culture of Japan. M.N. also thanks the Nishida Foundation for the Promotion of Basic Organic Chemistry for financial support.

References

[1] G.N. La Mar and F.A. Walker, in D. Dolphin (ed.), *The Porphyrins*, Vol. IV, Academic Press, New York, 1979, pp. 61–157.
[2] I. Bertini and C. Luchinat, in A.B.P. Lever and H.B. Gray (eds.), *NMR of Paramagnetic Molecules in Biological Systems*, Bejamin/Cummings, Menlo Park, CA, 1986, pp. 165–229.
[3] G. Palmer, in D. Dolphin (ed.), *The Porphyrins*, Vol. IV, Academic Press, New York, 1979, pp. 313–353.
[4] G. Palmer, in A.B.P. Lever and H.B. Gray (eds.), *Iron Porphyrins*, Part 2, Benjamin/Cummings, Menlo Park, CA, 1982, pp. 43–88.
[5] W.R. Scheidt and D.M. Chipman, *J. Am. Chem. Soc., 108* (1986) 1163.
[6] G.N. La Mar, K.M. Smith, K. Gersonde, H. Sick and M. Overkamp, *J. Biol. Chem., 255* (1980) 66.
[7] M. Smith and G. McLendon, *J. Am. Chem. Soc., 103* (1981) 4912.
[8] J.D. Satterlee, J.E. Erman, G.N. La Mar, K.M. Smith and K.C. Langry, *J. Am. chem. Soc., 105* (1983) 2099.
[9] Y. Yamamoto, N. Nanai, R. Chujo and T. Suzuki, *FEBS Lett., 264* (1990) 113.
[10] F.A. Walker, D. Reis and V.L. Balke, *J. Am. Chem. Soc., 106* (1984) 6888.
[11] R. Quinn, J.S. Valentine, M.P. Byrn and C.E. Strouse, *J. Am. Chem. Soc., 109* (1987) 3301.
[12] J.S. Leigh, Jr. and M. Erecinska, *Biochim. Biophys. Acta, 387* (1975) 95.
[13] C.T. Migita and M. Iwaizumi, *J. Am. Chem. Soc., 103* (1981) 4378.
[14] A. Tsai and G. Palmer, *Biochim. Biophys. Acta, 681* (1982) 484.
[15] J.C. Salerno, *J. Biol. Chem., 259* (1984) 2331.

[16] F.A. Walker, B.H. Huynh, W.R. Scheidt and S.R. Osvath, *J. Am. Chem. Soc., 108* (1986) 5288.
[17] D. Inniss, S.M. Soltis and C.E. Strouse, *J. Am. Chem. Soc., 110* (1988) 5644.
[18] K. Hatano, M.K. Safo, F.A. Walker and W.R. Scheidt, *Inorg. Chem., 30* (1991) 1643.
[19] T.G. Traylor and A.P. Berzinis, *J. Am. Chem. Soc., 102* (1980) 2844.
[20] H. Goff, *J. Am. Chem. Soc., 102* (1980) 3252.
[21] F.A. Walker, J. Buehler, J.T. West and J.L. Hinds, *J. Am. Chem. Soc., 105* (1983) 6923.
[22] R.M. Keller and K. Wuthrich, *Biochim. Biophys. Acta, 533* (1978) 195.
[23] R.M. Keller and K. Wuthrich, *Biochim. Biophys. Acta, 62* (1980) 204.
[24] H. Zhang, U. Simonis and F.A. Walker, *J. Am. Chem. Soc., 112* (1990) 6124.
[25] F.A. Walker, U. Simonis, H. Zhang, J.M. Walker, T.M. Ruscitti, C. Kipp, M.A. Amputch, B.V. Castillo III, S.H. Cody, D.L. Wilson, R.E. Graul, G.J. Yong, K. Tobin, J.T. West and B.A. Barichievich, *New J. Chem., 16* (1992) 609.
[26] M. Nakamura and J.T. Groves, *Tetrahedron, 44* (1988) 3225.
[27] M. Nakamura and N. Nakamura, *Chem. Lett.,* (1991) 627.
[28] H.E. Baumgarten (ed. in chief), *Organic Syntheses,* Coll. Vol. 5, Wiley, New York, 1973, p. 365.
[29] H.E. Baumgarten (ed. in chief), *Organic Syntheses,* Coll. Vol. 5, Wiley, New York, 1973, p. 49.
[30] T. Matuura and M. Inokai, *Kogyo Kagaku Zasshi, 72* (1969) 179.
[31] R.W. Wagner, D.S. Lawrence and J.S. Lindsey, *Tetrahedron Lett., 28* (1987) 3069.
[32] J.S. Lindsey and R.W. Wagner, *J. Org. Chem., 54* (1989) 828.
[33] A.D. Adler, F.R. Longo, F. Kampas and J. Kim, *Inorg. Nucl. Chem., 32* (1970) 2443.
[34] J.T. Groves and T.E. Nemo, *J. Am. Chem. Soc., 105* (1983) 6243.
[35] A.L. Van Geet, *Anal. Chem., 42* (1970) 679.
[36] J.D. Satterlee, G.N. La Mar and T.J. Bold, *J. Am. Chem. Soc., 99* (1977) 1088.
[37] T. Yoshimura and T. Ozaki, *Bull. Chem. Soc. Jpn., 52* (1979) 2268.
[38] F.A. Walker, M.-W. Lo and M.T. Ree, *J. Am. Chem. Soc., 98* (1976) 5552.
[39] M. Nakamura, *Inorg. Chim. Acta, 161* (1989) 73.
[40] M. Nakamura and N. Nakamura, *Chem. Lett.,* (1991) 1885.
[41] M. Nishio and M. Hirota, *Tetrahedron, 45* (1989) 7201.
[42] H. Imai, S. Nakagawa and E. Kyuno, *J. Am. Chem. Soc., 114* (1992) 6719.
[43] M. Nakamura and N. Nakamura, *Chem. Lett.,* (1990) 181.
[44] F.A. Walker and U. Simonis, *J. Am. Chem. Soc., 113* (1991) 8652.
[45] W.R. Scheidt, J.F. Kirner, J.L. Hoard and C.A. Reed, *J. Am. Chem. Soc., 109* (1987) 1963.
[46] M.K. Safo, G.P. Gupta, F.A. Walker and W.R. Scheidt, *J. Am. Chem. Soc., 113* (1991) 5497.
[47] K.M. Barkigia, M.D. Berber, J. Fajer, C.J. Medforth, M.W. Renner and K.M. Smith, *J. Am. Chem. Soc., 112* (1990) 8851.
[48] S. Forsen and R.A. Hoffman, *J. Chem. Phys., 39* (1963) 2892.
[49] V. Thanabal, J.S. de Ropp and G.N. La Mar, *J. Am. Chem. Soc., 109* (1987) 7516.
[50] J. Sandstrom, *Dynamic NMR Spectroscopy,* Academic Press, London, 1982.
[51] M. Nakamura, *Chem. Lett.,* (1992) 2423.
[52] G.N. La Mar and F.A. Walker, *J. Am. Chem. Soc., 95* (1973) 1782.
[53] M.K. Safo, G.P. Gupta, C.T. Watson, U. Simonis, F.A. Walker and W.R. Scheidt, *J. Am. Chem. Soc., 114* (1992) 7066.
[54] A. Albert, *Phys. Methods Heterocycl. Chem., 1* (1963) 1.
[55] G.N. La Mar, T.J. Bold and J.D. Satterlee, *Biochim. Biophys. Acta, 498* (1977) 189.
[56] W.R. Scheidt, S.R. Osvath and Y.J. Lee, *J. Am. Chem. Soc., 109* (1987) 1958.
[57] T.B. Higgins, M.K. Safo and W.R. Scheidt, *Inorg. Chim. Acta, 178* (1990) 261.
[58] H.M. Goff, *J. Am. Chem. Soc., 103* (1981) 3714.
[59] M. Oki, *Application of Dynamic NMR Spectroscopy to Organic Chemistry,* VCH, Deerfield Beach, FL, 1985, pp. 1–40.